Supporting information

Ligated Solvent Influence on Interpenetration and Carbon Dioxide and Water Sorption Hysteresis in a System of 2D Isoreticular MOFs

Nabanita Chatterjee and Clive L. Oliver*

Department of Chemistry, University of Cape Town, Rondebosch, 7701, South Africa
E-mail: Clive.Oliver@uct.ac.za (Dr Clive L. Oliver)

Table S1. Crystal data and refinement parameters for **1**, **2**, **3** and **4**.

	1	**2**	**3**	**4**
ASU formula	$C_{20.75}H_{16.75}CuF_6N_{1.25}O_{5.25}$	$C_{22}H_{19}CuF_6NO_5$	$C_{87}H_{105}Cu_3F_{18}N_9O_{23}$	$C_{41}H_{32}Cu_2F_{12}NO_9$
Formula weight	545.14	554.92	2177.41	1037.75
Temperature / K	100(2)	100(2)	100(2)	298(2)
Crystal system	monoclinic	monoclinic	monoclinic	monoclinic
Space group	*C*2/*c*	*C*2/*c*	$P2_1/n$	$P2_1$
a / Å	31.972(4)	33.4847(19)	15.9401(11)	13.6525(6)
b /Å	7.2541(9)	7.2950(4)	30.5267(18)	10.8401(5)
c / Å	23.023(3)	23.6806(15)	20.6516(15)	24.9143(10)
β / °	119.895(3)	122.127(2)	93.306(2)	101.1070(10)
Volume / $Å^3$	4629.3(10)	4898.7(5)	10032.3(12)	3618.1(3)
Z	8	8	4	2
ρ_{calc} / g cm^{-3}	1.564	1.505	1.442	0.953
μ / mm^{-1}	1.025	0.969	0.736	1.301
F(000)	2200.0	2248.0	4492.0	1046.0
Crystal size/mm^3	0.55 × 0.43 × 0.18	0.31 × 0.24 × 0.22	0.14 × 0.15 × 0.24	0.36 × 0.34 × 0.15
Radiation	MoKα (λ = 0.71073)	MoKα (λ = 0.71073)	MoKα (λ = 0.71073)	CuKα (λ = 1.54178)
2θ range for data collection / °	3.652 to 61.082	5.746 to 53.732	2.384 to 61.444	6.886 to 149.76
Index ranges	-45 ≤ h ≤ 45, -10 ≤ k ≤ 10, -32 ≤ l ≤ 32	-42 ≤ h ≤ 40, -9 ≤ k ≤ 8, -29 ≤ l ≤ 30	-22 ≤ h ≤ 22, -28 ≤ k ≤ 43, -29 ≤ l ≤ 29	-17 ≤ h ≤ 16, 0 ≤ k ≤ 13, 0 ≤ l ≤ 31
Reflections collected	38885	20411	136725	7682
Independent reflections	7072 [R_{int} = 0.0252, R_{sigma} = 0.0197]	5221 [R_{int} = 0.0361, R_{sigma} = 0.0318]	30851 [R_{int} = 0.0652, R_{sigma} = 0.0591]	7682 [R_{int} = 0.0476, R_{sigma} = 0.0420]
Data/restraints/parameters	7072/0/312	5221/0/318	30851/345/1302	7682/189/650
Goodness-of-fit on F^2	1.057	1.238	1.098	1.377
Final R indexes [I>=2σ (I)]	R_1 = 0.0681, wR_2 = 0.2009	R_1 = 0.0399, wR_2 = 0.1459	R_1 = 0.1202, wR_2 = 0.3053	R_1 = 0.0938, wR_2 = 0.2742
Final R indexes [all data]	R_1 = 0.0810, wR_2 = 0.2154	R_1 = 0.0434, wR_2 = 0.1493	R_1 = 0.1561, wR_2 = 0.3319	R_1 = 0.0959, wR_2 = 0.2808
Largest diff. peak/hole / e $Å^{-3}$	2.31/-0.75	0.72/-0.50	5.94/-1.72	1.20/-0.65

(a)

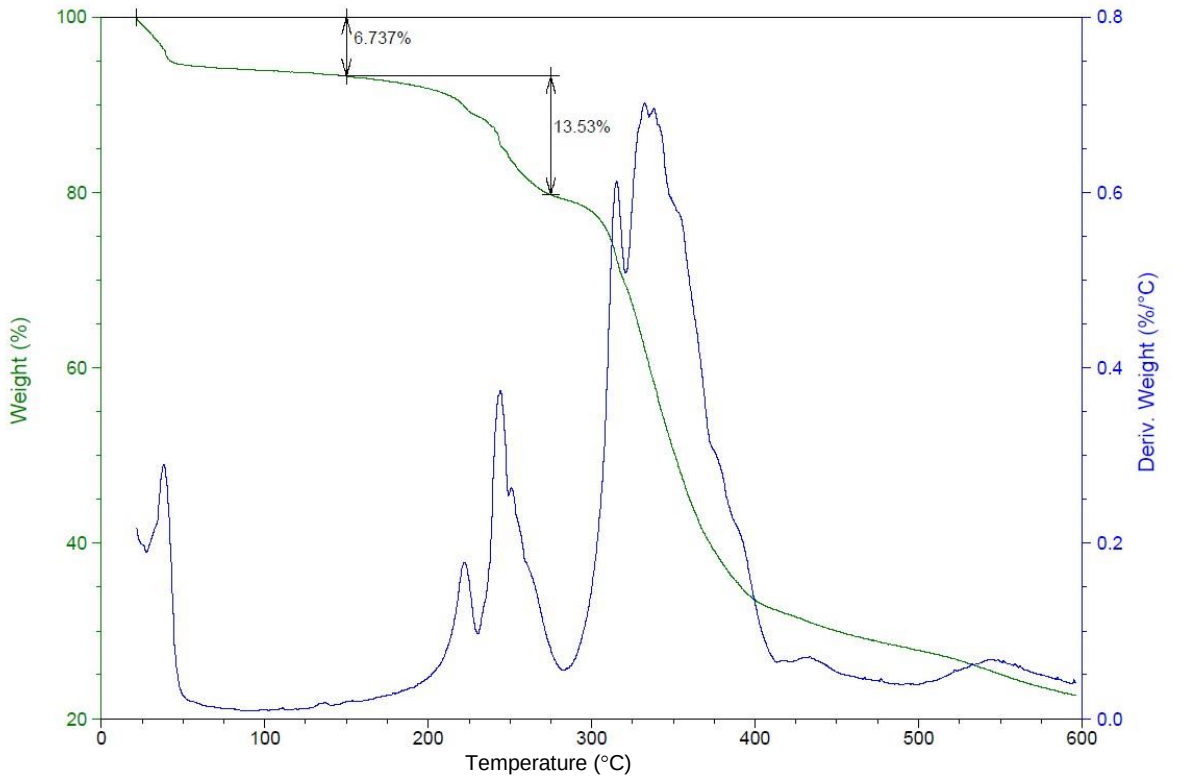

(b)

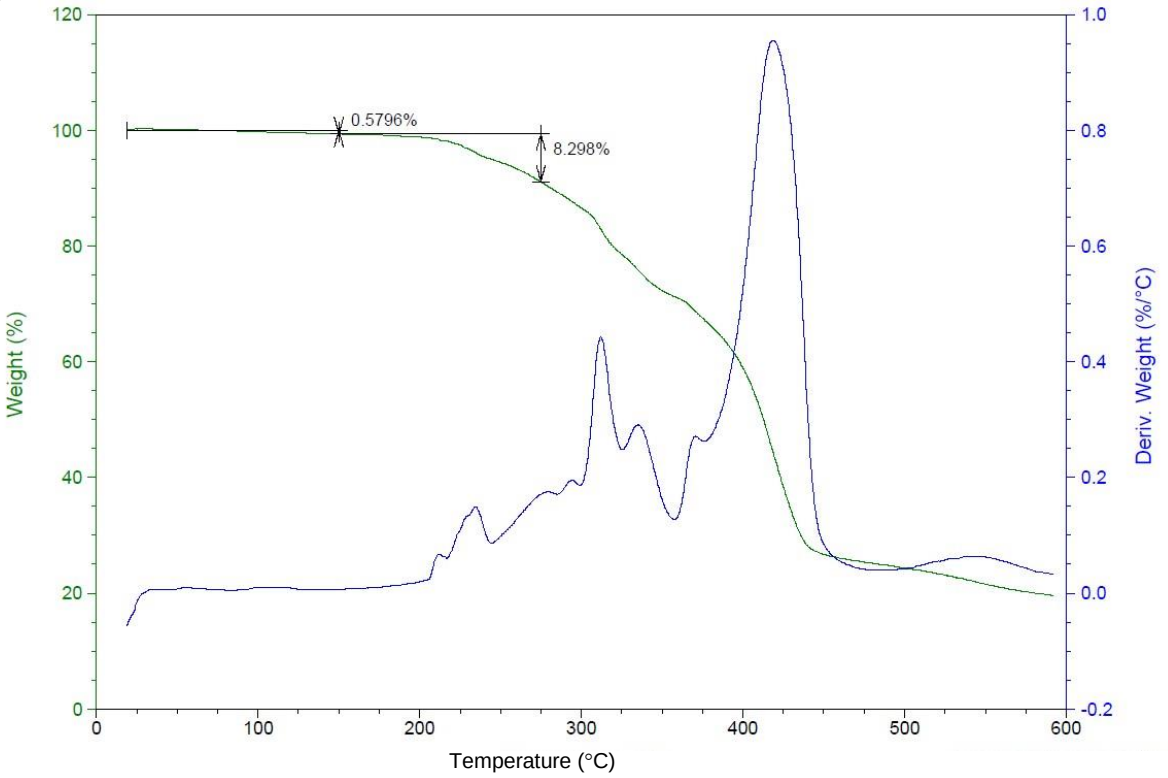

Figure S1. TGA graphs of weight % vs temperature (in green) and the first derivative of weight % with respect to temperature (in blue) for (a) **1** and (b) **2**.

(a)

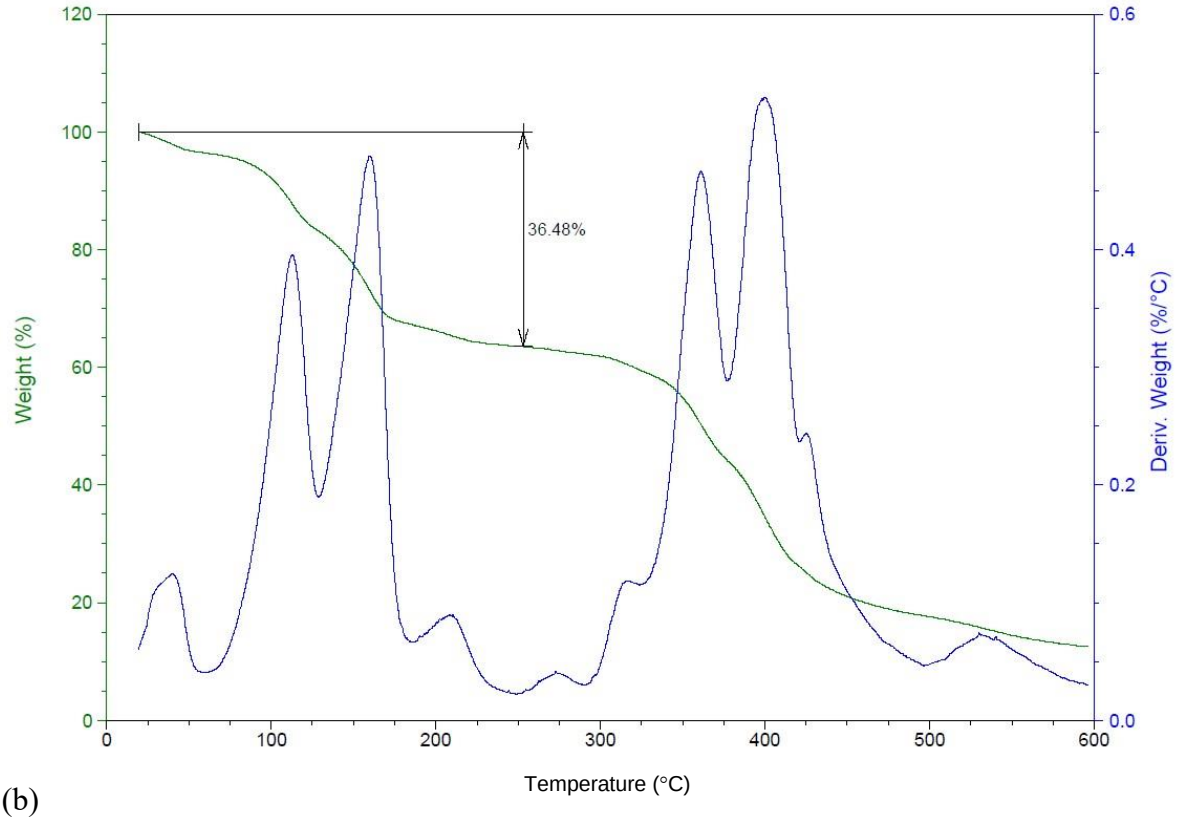

(b)

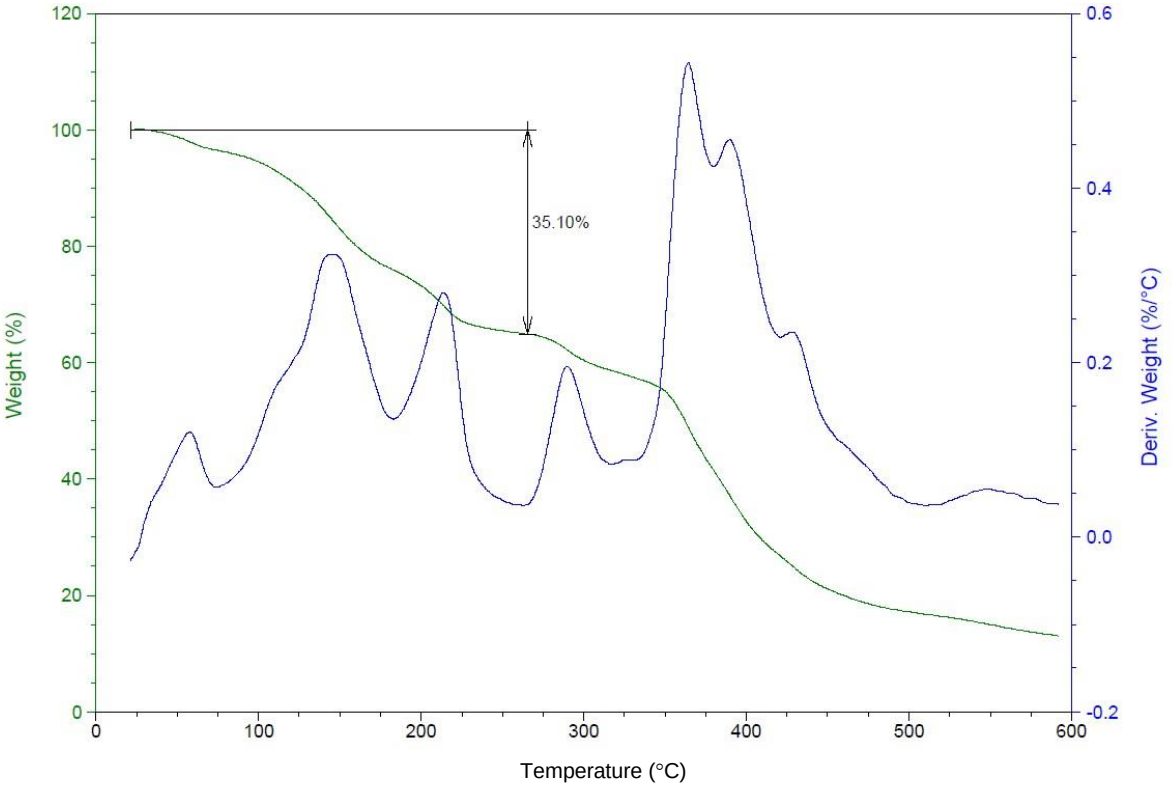

Figure S2. TGA graphs of weight % vs temperature (in green) and the first derivative of weight % with respect to temperature (in blue) for (a) **3** and (b) **4**.

(a)

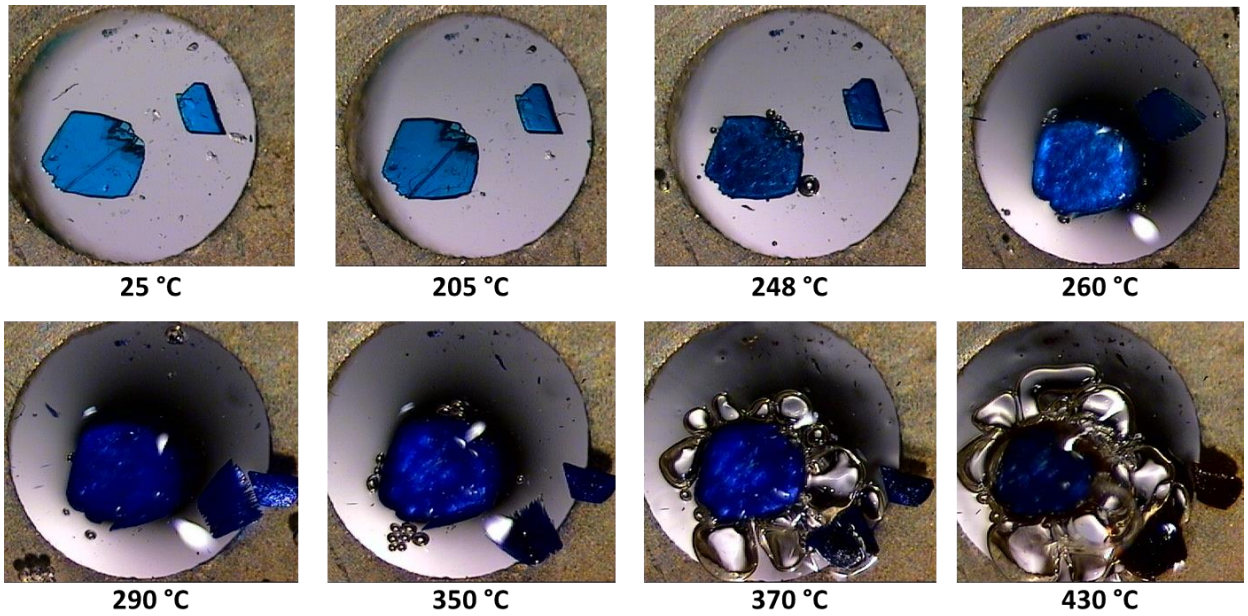

(b)

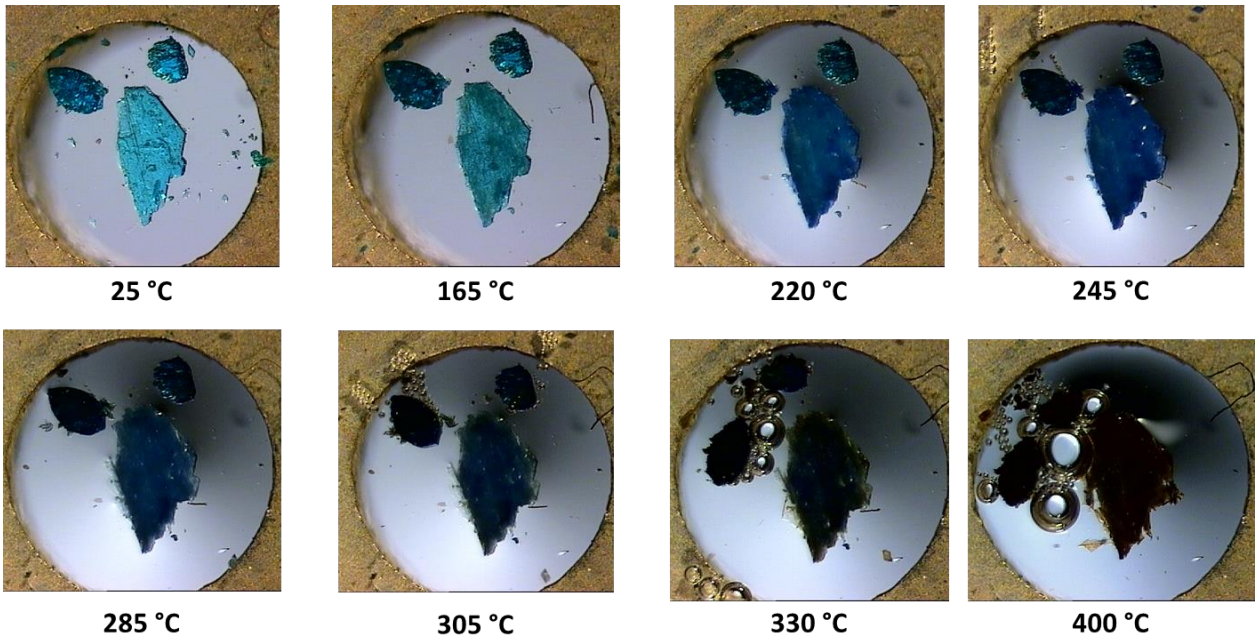

Figure S3. Hot stage microscopy images of (a) **1** and (b) **2** from 25ºC to 400-430 ºC.

(a)

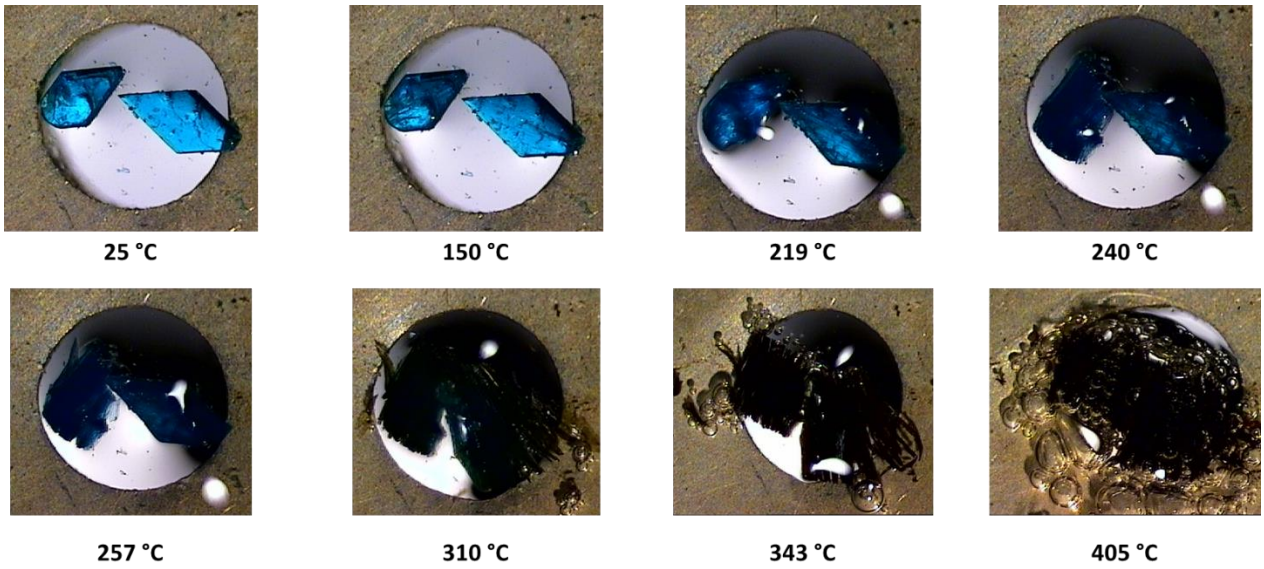

(b)

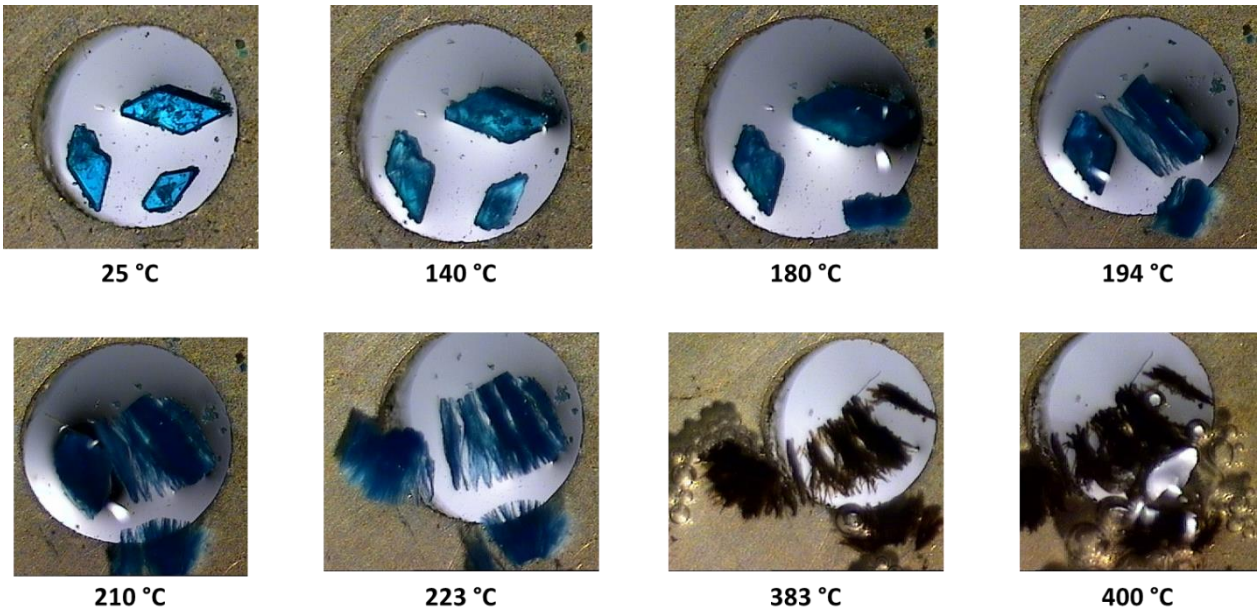

Figure S4. Hot stage microscopy images of (a) **3** and (b) **4** from 25ºC to ~400ºC.

(a)

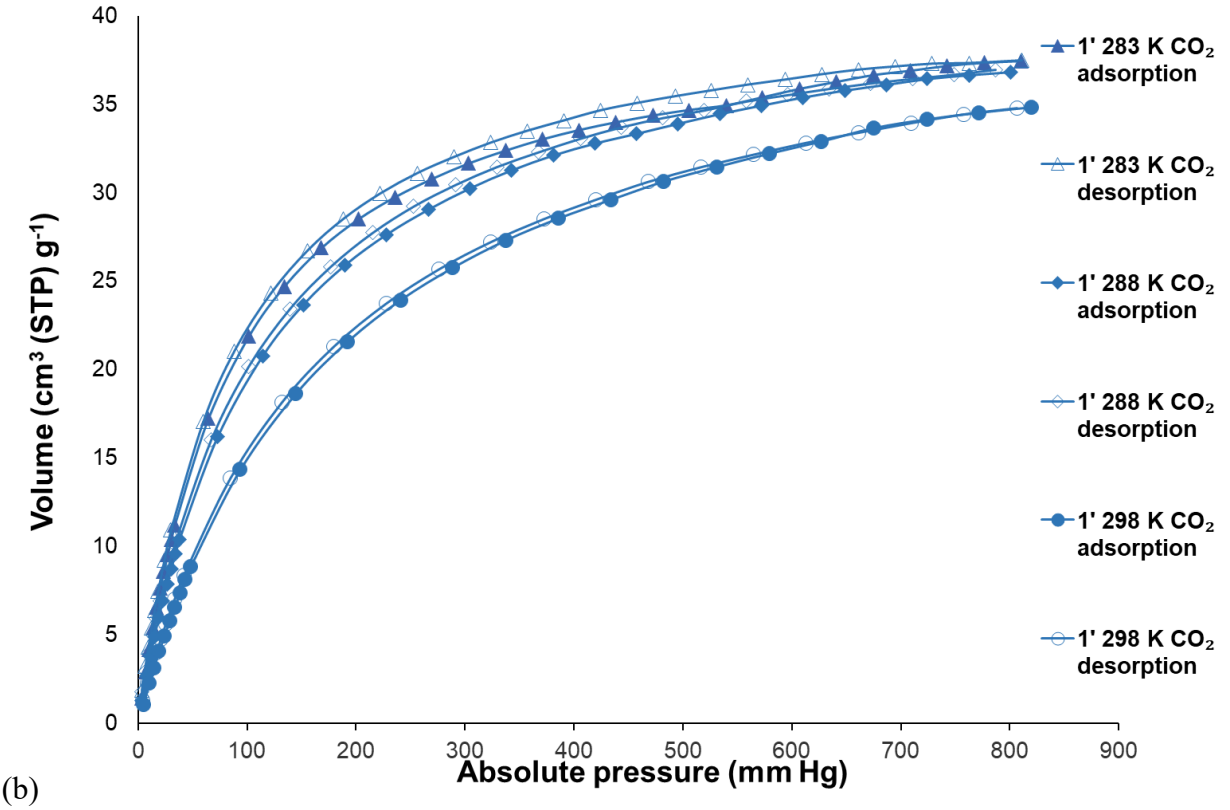

(b)

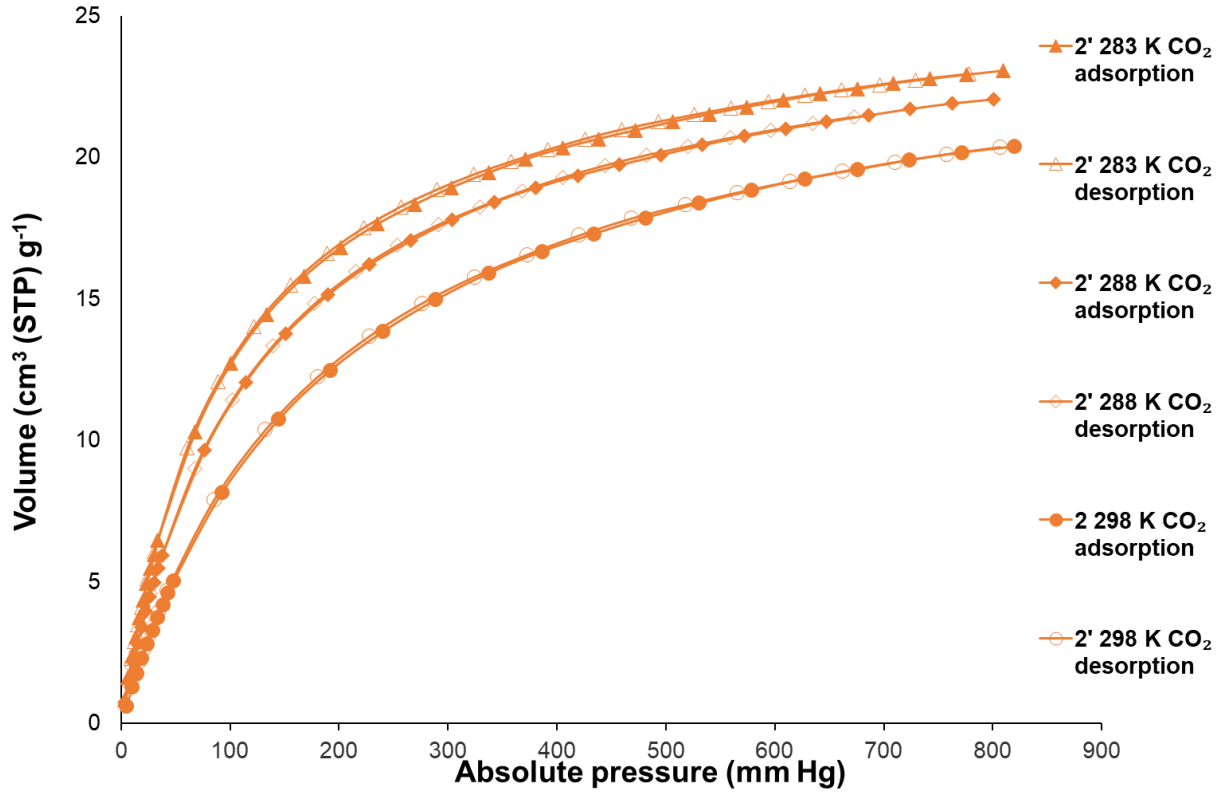

Figure S5. CO_2 adsorption and desorption isotherms for (a) **1′** and (b) **2′** between 283 – 298 K.

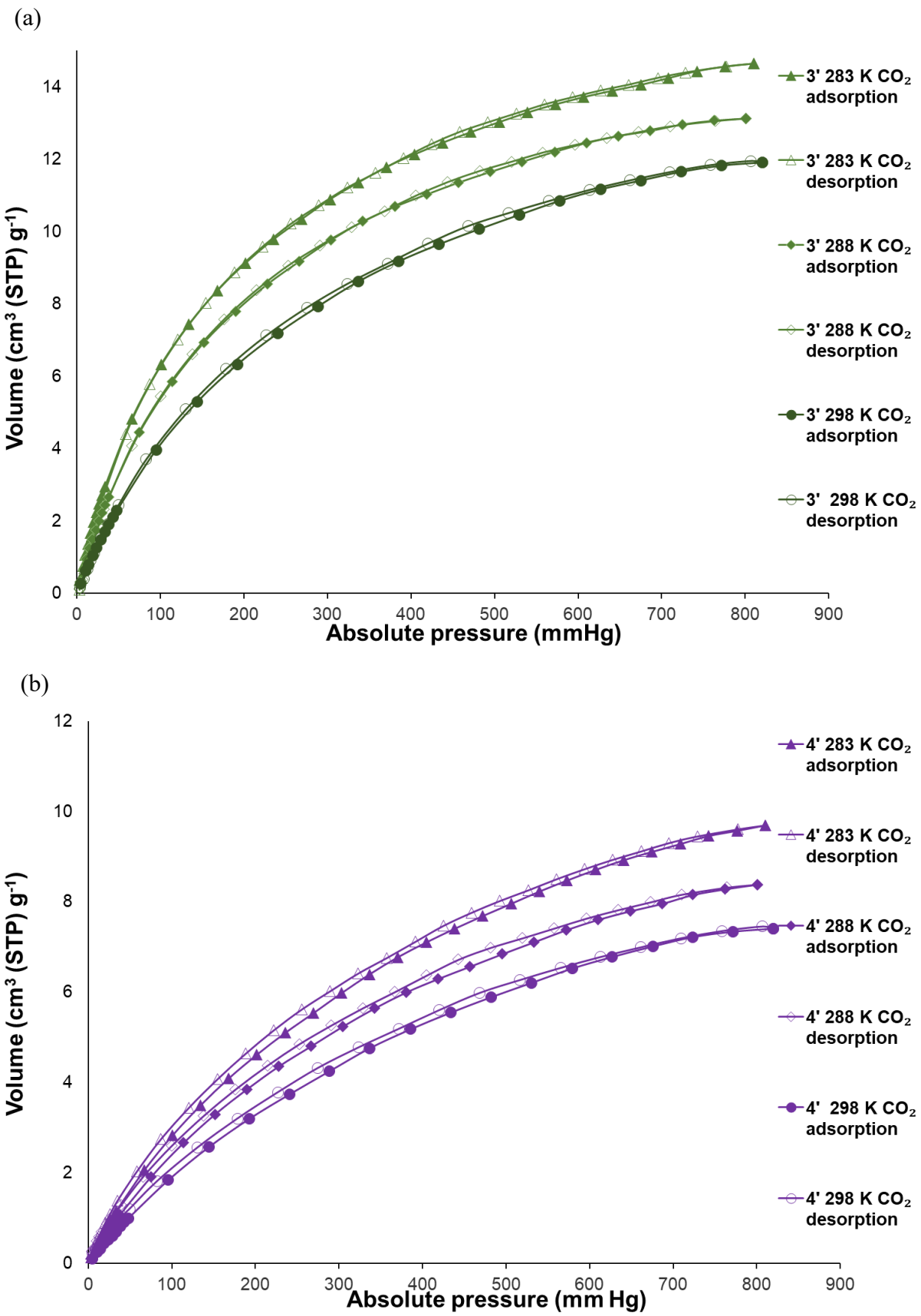

Figure S6. CO_2 adsorption and desorption isotherms for (a) **3′** and (b) **4′** between 283 – 298 K.

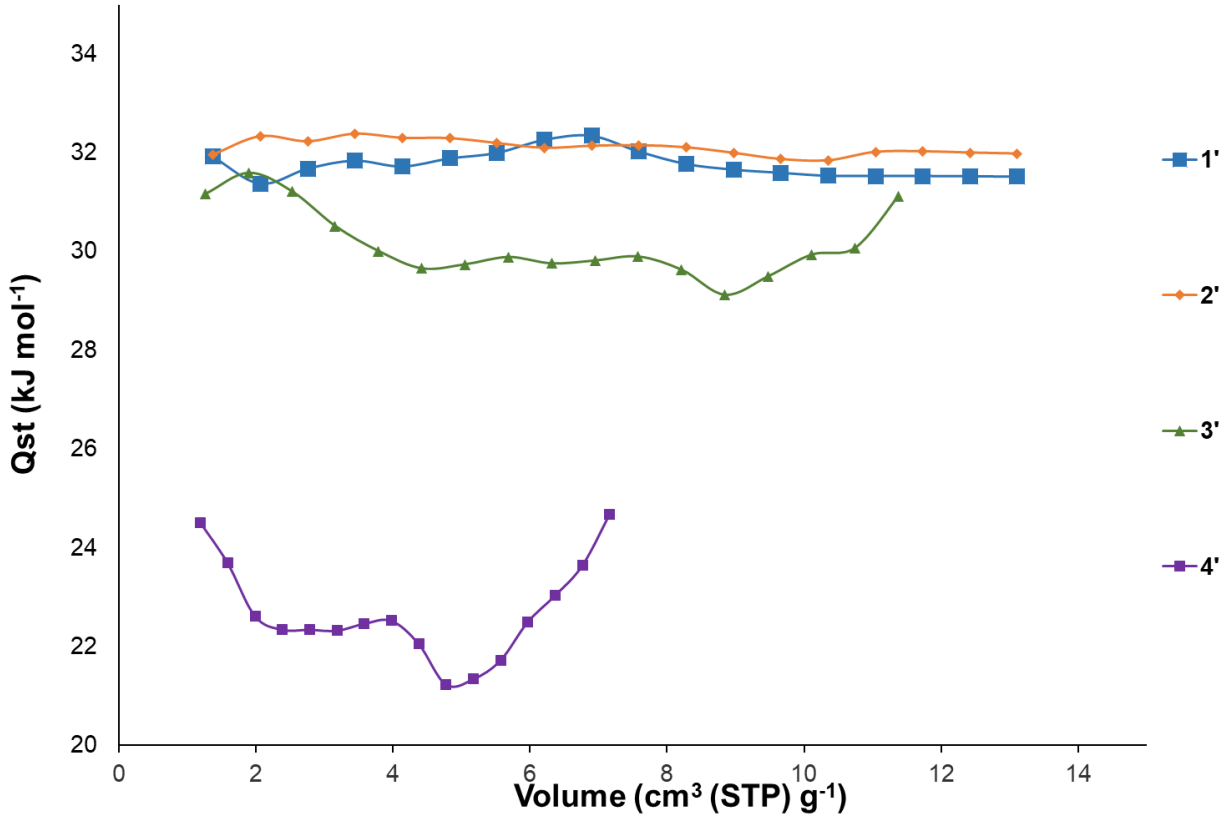

Figure S7. Q_{st} values of **1′-4′** in various loading ranges using isotherms from 283-298 K. Note that since the 298 K isotherms have the lowest sorption, that the maxima of the load ranges are determined by maxima of the 298 K isotherms for each activated MOF.

Table S2. Crystal data and refinement parameters for **1**, **1W**, **1W′** and **1W′R**.

	1	**1W**	**1W′**	**1W′R**
ASU formula	$C_{20.75}H_{16.75}CuF_6N_{1.25}O_{5.25}$	$C_{17.75}H_{11.75}CuF_6N_{0.25}O_{5.25}$	$C_{17}H_8CuF_6O_4$	$C_{17}H_{10}CuF_6O_5$
Formula weight	545.14	490.06	453.77	471.79
Temperature / K	100(2)	100.0	100.0	298.0
Crystal system	monoclinic	monoclinic	monoclinic	monoclinic
Space group	*C*2/*c*	*P*2/*n*	*P*2/*n*	*P*2/n
a / Å	31.972(4)	12.7688(12)	12.478(2)	12.816(5)
b /Å	7.2541(9)	6.9836(7)	6.9904(12)	7.019(3)
c / Å	23.023(3)	20.709(2)	20.411(4)	20.866(8)
β / °	119.895(3)	94.226(2)	90.633(4)	94.224(7)
Volume / $Å^3$	4629.3(10)	1841.7(3)	1780.4(5)	1871.9(12)
Z	8	4	4	4
ρ_{calc} / g cm^{-3}	1.564	1.767	1.693	1.674
μ / mm^{-1}	1.025	1.276	1.307	1.251
F(000)	2200.0	980.0	900.0	940.0
Crystal size/mm^3	0.55 × 0.43 × 0.18	0.61 × 0.4 × 0.12	0.61 × 0.4 × 0.12	0.61 × 0.4 × 0.12
Radiation	MoKα (λ = 0.71073)	MoKα (λ = 0.71073)	MoKα (λ =	MoKα (λ = 0.71073)
2θ range for data collection / °	3.652 to 61.082	3.632 to 60.848	3.806 to 60.892	3.614 to 61.538
Index ranges	-45 ≤ h ≤ 45, -10 ≤ k ≤ 10, -32 ≤ l ≤ 32	-18 ≤ h ≤ 18, 0 ≤ k ≤ 9, 0 ≤ l ≤ 29	-17 ≤ h ≤ 17, 0 ≤ k ≤ 9, 0 ≤ l ≤ 29	-18 ≤ h ≤ 17, 0 ≤ k ≤ 9, 0 ≤ l ≤ 29
Reflections collected	38885	5407	4985	5256
Independent reflections	7072 [R_{int} = 0.0252, R_{sigma} = 0.0197]	5407 [R_{int} = 0.0447, R_{sigma} = 0.1224]	4985 [R_{int} = 0.0630, R_{sigma} = 0.1088]	5256 [R_{int} = 0.0700, R_{sigma} = 0.1473]
Data/restraints/parameters	7072/0/312	5407/48/301	4985/0/254	5256/0/264
Goodness-of-fit on F^2	1.057	1.037	1.148	0.989
Final R indexes [I>=2σ (I)]	R_1 = 0.0681, wR_2 = 0.2009	R_1 = 0.0806, wR_2 = 0.2118	R_1 = 0.0819, wR_2 = 0.1899	R_1 = 0.0840, wR_2 = 0.2054
Final R indexes [all data]	R_1 = 0.0810, wR_2 = 0.2154	R_1 = 0.1334, wR_2 = 0.2362	R_1 = 0.1375, wR_2 = 0.2163	R_1 = 0.1630, wR_2 = 0.2488
Largest diff. peak/hole / e $Å^{-3}$	2.31/-0.75	2.04/-1.12	1.89/-1.02	1.36/-1.11

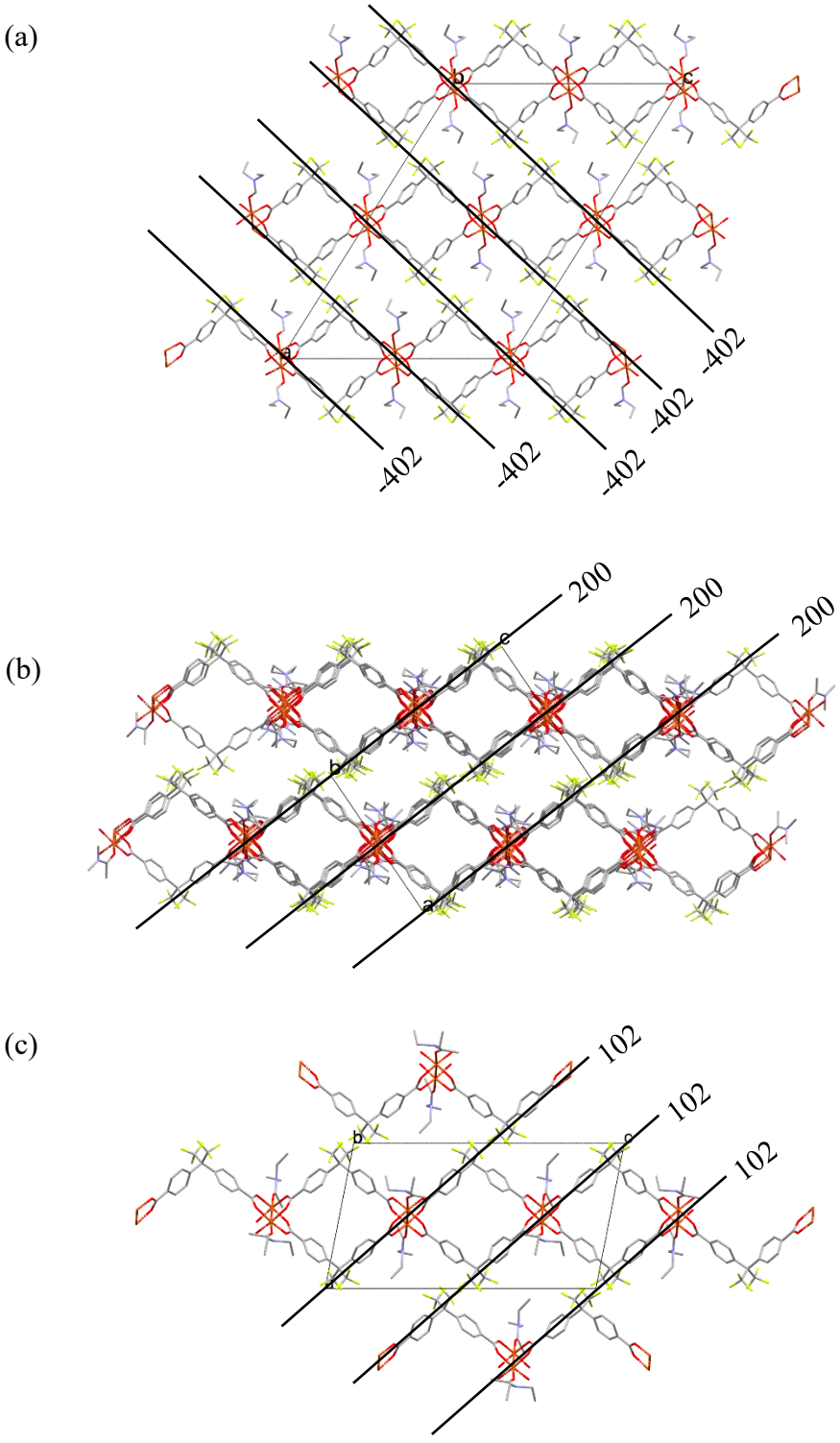

Figure S8. Structurally equivalent planes in (a) **2** (-402) (b) **3** (200) and (c) **4** (102) close to which the trifuoromethyl groups of all 2D layers reside. Desolvation will cause the trifluoromethyl groups of alternative layers to move orthogonal to these reference planes which will cause destructive interference of X-rays causing these peaks to become absent in the PXRD patterns.

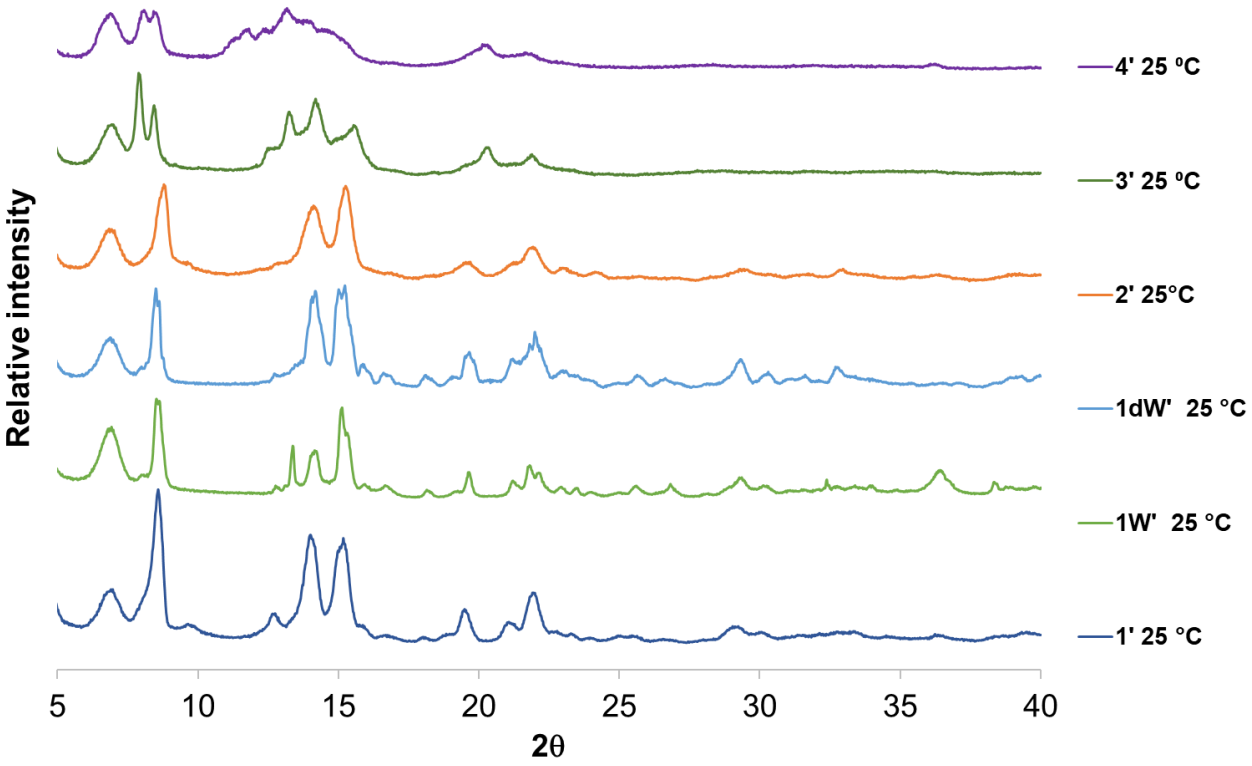

Figure S9. Return-to-25ºC variable-temperature PXRD patterns (under vacuum) of **1′**, **1W′**, **1dW′**, **2′**, **3′** and **4′**.

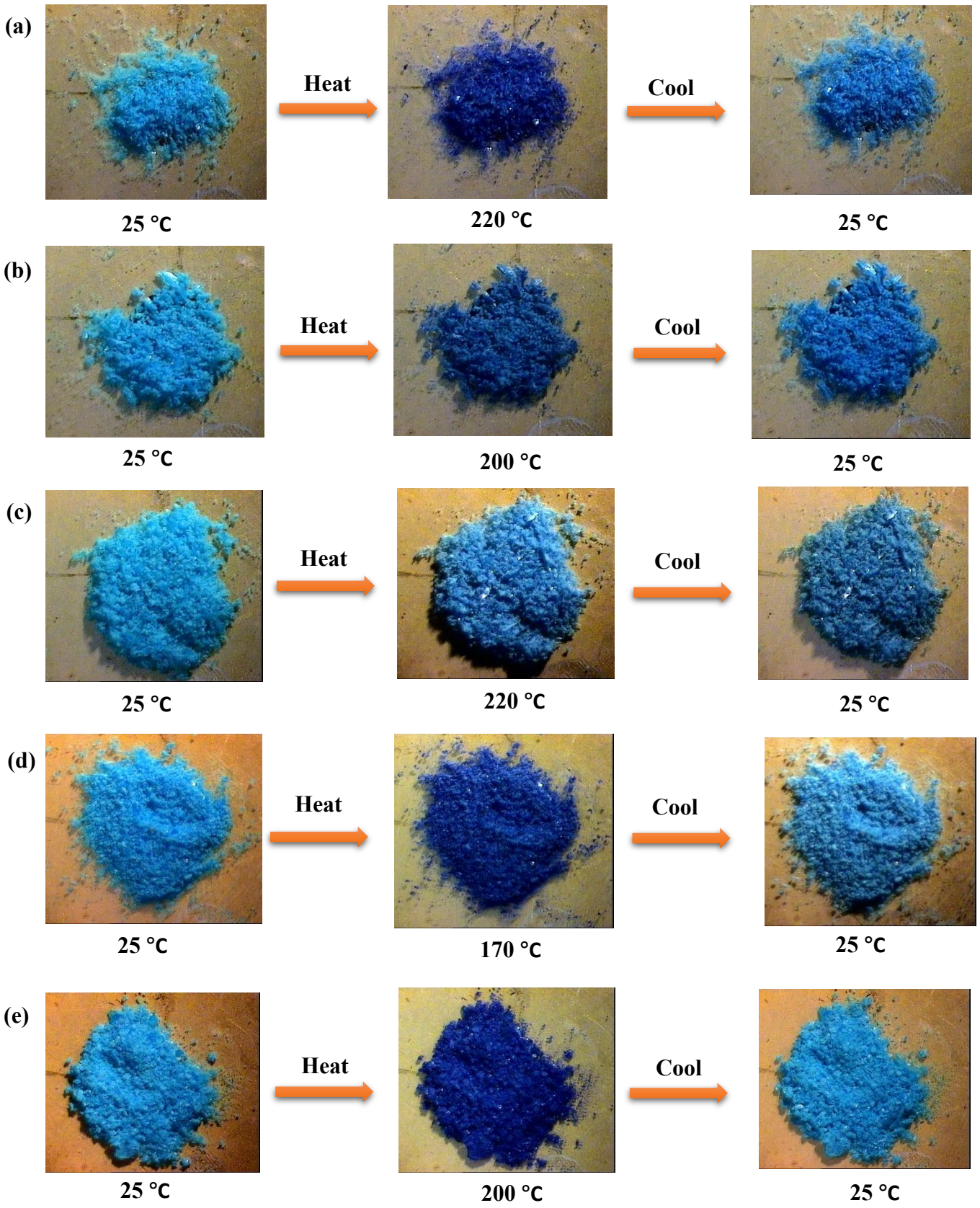

Figure S10. Color changes in powders of (a) **2** (b) **3** (c) **4** (d) **1W** and (e) **1** after desolvation and subsequent adsorption of atmospheric water upon cooling.

Extent of hysteresis

The extent of hysteresis (EH) was calculated according to the Barbour et. al formula (Equation S1) and Sapchenko et. al formula (Equation S2).[1, 2]

$$EH = \frac{\text{Area of desorption} - \text{Area of adsorption}}{\text{Area of desorption}} \qquad \text{…… Equation S1}$$

$$EH = \frac{\text{Area of desorption} - \text{Area of adsorption}}{\text{Area of adsorption}} \qquad \text{…… Equation S2}$$

Experimental procedure S1: Preparation of [Cu(hfipbb)(H_2O)]$_n$ (1dW)

4,4′-(hexafluoroisopropylidene)bis(benzoic acid) (H_2hfipbb) (114 mg, 0.29 mmol) were dissolved in 1 mL *N*,*N*′-dimethylacetamide (DMA). In a separate vial, copper nitrate trihydrate (75 mg, 0.31 mmol) was dissolved in 1 mL water after which the metal salt and ligand solutions were mixed at room temperature. A capped vial, containing the combined solutions, was then heated at 90 °C for 2 d, after which it was allowed to cool slowly to room temperature yielding block shape deep blue crystals of **1dW**.

References

(1) Lama, P.; Aggarwal, H.; Bezuidenhout, C. X.; Barbour, L. J. Giant Hysteretic Sorption of CO_2: In Situ Crystallographic Visualization of Guest Binding within a Breathing Framework at 298 K. *Angewandte Chemie-International Edition* **2016**, *55*, 13271-13275.

(2) Sapchenko, S. A.; Barsukova, M. O.; Belosludov, R. V.; Kovalenko, K. A.; Samsonenko, D. G.; Poryvaev, A. S.; Sheveleva, A. M.; Fedin, M. V.; Bogomyakov, A. S.; Dybtsev, D. N.; Schröder, M.; Fedin, V. P. Understanding Hysteresis in Carbon Dioxide Sorption in Porous Metal–Organic Frameworks. *Inorg. Chem.* **2019**, *58*, 6811-6820.